Supporting Information

Electrophilic Molecule-Induced π-π Interactions Reduce Energy Disorder of Hole Transport Layer for Highly Efficient Perovskite Solar Modules

Lei Wang[1], Shihao Yuan[1,*], Feng Qian[1], Ting Zhang[1], Hualin Zheng[2], Xiaobo Li[1], Tianyu Lan[1], Qien Xu[1], Peng Zhang[3], Shibin Li[1,*]

[1]School of Optoelectronic Science and Engineering, University of Electronic Science and Technology of China, Chengdu 610054, China.

[2]College of Optoelectronic Engineering, Chengdu University of Information Technology, Chengdu 610225, China

[3]College of Optical and Electronic Technology, China Jiliang University, Hangzhou 310018, China

*Correspondence: yuanshihao@uestc.edu.cn, shibinli@uestc.edu.cn

Experimental Section

Materials: All chemicals and solvents were used as received without further purification. Formamidine hydroiodide (FAI, 99.9%), cesium iodide (CsI, 99.999%), lead (II) iodide (PbI_2, 99.999%), lead (II) bromide ($PbBr_2$, 99.99%), Methylammonium Chloride (MACl, 99.9%), [4-(3,6-dimethyl-9H-carbazol-9-yl)butyl]phosphonic acid (Me-4PACZ) and bathocuproine (BCP) were purchased from Xi'an Polymer Light Technology corp. C_{60} was purchased from Luminescence Technology Corp. Chlorobenzene (CB, anhydrous, 99.8%) was obtained from Advanced Election Technology CO.，Ltd. Dimethylformamide (DMF, 99.8%), 1-Methyl-2-pyrrolidinone

(NMP, 99%), 2,6-Difluorobenzonitrile (FCN), 2,4-Difluoronitrobenzene (FNO_2) and 2,6-Difluoro-3-nitrobenzonitrile ($FCNO_2$) were purchased from Sigma-Aldrich.

Device Fabrication: ITO glass substrates were cleaned with acetone, deionized water and anhydrous ethanol successively, and each ultrasonic cleaning time was 15min. For preparation of hole transport layer (HTL) NiO_x, the NiO_x layer was radio-frequency (RF)-sputtered onto the pre-cleaned ITO glass substrates (ultraviolet ozone treatment for 20 min) at room temperature with a chamber pressure of 0.37Pa, RF power of 200 W, argon flow rate of 100 sccm for 30 min. The sputtered NiO_x films were annealed at 300 °C for 30 min under ambient conditions. The PTAA modified layer was formed by doping FCN, FNO_2 and $FCNO_2$ molecules (0-0.3 mg/ml) into PTAA (1 mg/mL in chlorobenzene) to form a mixed solution, which was then spin-coated onto the NiOx substrate at 4000 rpm for 30 s. For $Cs_{0.05}FA_{0.95}Pb(Br_{0.05}I_{0.95})_3$ perovskite films, 1.6 M perovskite precursor solution was prepared by dissolving FAI, PbI_2, CsI, $PbBr_2$ and MACl (0.3 mmol) in mixed solvents of DMF and NMP (v/v: 6:1). The filtered perovskite precursor solution was spin-coated on substrates at 4500 rpm for 7 s, and then the perovskite wet film was quickly transferred to the sample chamber connected to the vacuum pump. The vacuum pump was turned on, and the perovskite film was immediately exposed to a low pressure of 10 Pa for 25 seconds. Subsequently, the resulting perovskite films were annealed at 100 °C for 20 min in air. Then, C_{60} (30 nm), BCP (6 nm) were sequentially thermally evaporated onto the perovskite films in a vacuum chamber ($< 5\times10^{-4}$ Pa). Finally, a 100 nm Cu electrode was thermally evaporated on the BCP film.

For the 10×10 cm^2 solar module, the FTO cleaning process is the same as above, the red laser of 1064 nm was used to scribe the 10×10 cm^2 FTO substrate to form 11 strips (P1). The preparation of NiO_x layer is consistent with the method of small device. The $FCNO_2$-incorporated PTAA layer was blade-coated with a blade gap of 180 μm above the NiO_x layer at a speed of 20 mm/s or the $FCNO_2$-incorporated Me-4PACZ layer (1mg/mL in anhydrous ethanol) was blade-coated with a blade gap of 180 μm above the NiO_x layer at a speed of 40 mm/s. For $Cs_{0.05}FA_{0.95}Pb(Br_{0.05}I_{0.95})_3$ perovskite films, 1 M perovskite precursor solution was coated on HTL substrate by slot-die method with a gap between the slip and the coated substrate of 200 μm, a feed pump speed of 0.6 μl/s, and a substrate moving speed of 6000 μm/s. The perovskite wet film was quickly transferred to the sample chamber connected to the vacuum pump. The vacuum pump was turned on, and the perovskite film was immediately exposed to a low pressure of 10 Pa for 40 seconds. Subsequently, the resulting perovskite films were annealed at 100 °C for 25 min in air. Then, C_{60} (55 nm), BCP (8.5 nm) were sequentially thermally evaporated onto the perovskite films in a vacuum chamber (< 5×10^{-4} Pa) and a green laser of 532 nm (P2) was used to etched the obtained perovskite/C_{60}/BCP films. Finally, a 200 nm Cu electrode was thermally evaporated on the BCP film in a vacuum chamber (< 3×10^{-4} Pa) and the Cu electrode was divided by the green laser of 532 nm with a line width of 350 μm (P3). The modules fabricated on 10×10 cm^2 perovskite solar modules with an effective area of 57.3 cm^2 contain 11 series connected cells with a GFF of 89%.

Characterizations. The temperature dependence of hole mobility was measured by using a Keithley 4200-SCS semiconductor parameter analyzer. Fourier Transform Infrared (FT-IR) spectroscopy was recorded using a Thermo Fisher Scientific Nicolet iS50 in a wavelength range of 4000 to 650 cm^{-1}. Raman spectra were measured on a Horiba HR Evolution in a wavelength range of 2000 to 150 cm-1. Photoluminescence (PL) spectra and Time-resolved photoluminescence (TRPL) were acquired by employing the FLS980 Series of Fluorescence Spectrometers with an excitation wavelength of 480 nm. The UPS spectra were performed using Escalab 250Xi. X-ray photoelectron spectra (XPS) measurements were carried out on ESCALAB 250Xi. The roughness of films was measured using S NEOX 090 and contact angles of HTL films were measured using XG-CAMA1. The X-ray diffraction (XRD) was conducted using an X-ray diffractometer (Ultima IV) with Cu Kα radiation (λ=1.54 Å) at a scan speed of 5° min^{-1}. The Scanning Electron Microscopy (SEM) images and energy-dispersive spectroscopy (EDS) mapping were obtained via the field-emission scanning electron microscope (JEOL 7610F) using secondary electrons. Electrochemical impedance spectroscopy (EIS) was measured on an Electrochemical Workstation (China) and the data were processed using Z-View program. *J–V* curves of the perovskite solar cells were measured with a Keithley 2400 source meter under simulated solar illumination at 100 mW cm^{-2}, AM 1.5G standard air mass sunlight (Newport, Oriel Class A, 91195A), with anti-reflecting coating layers applied. The simulated light intensity was calibrated by a Si-reference cell. *J–V* curves were measured by reverse scan (from 1.2 V to -0.1 V) and forward scan (from -0.1 V to 1.2 V), where the scanning rate is 0.1V/s.

The black metal mask was used to define the effective active area of devices (0.08 cm^2). The module *J–V* curves were measured under the same environmental conditions, and the scan voltage changed to 13 V for 11 sub-cells modules, where the scanning rate is 0.8 V/s. External quantum efficiency (EQE) were characterized under monochromatic illumination (Oriel Cornerstone 260 1/4 m monochromator equipped with an Oriel 70613NS QTH lamp, Enlitech Co., Ltd). The steady-state power conversion efficiency was calculated by measuring the stable photocurrent density at a constant bias voltage (Vmax point).

Supplementary Note 1

The hole mobility calculation method

The hole mobility is calculated by fitting the *J-V* curve using the Mott-Gurney law.

$$J = \frac{9\varepsilon_0\varepsilon_r V^2}{8L^3} \quad (1)$$

where *J* represents the current density, ε_0 represents the vacuum permittivity, ε_r represents the dielectric constant of the NiO_x/PTAA, *V* represents the voltage applied to the device, and L represents the thickness of the NiO_x/PTAA layer.

Supplementary Note 2

The extent of density-of-states (DOS) calculation method

The extent of DOS is calculated by Gaussian fitting of the low-energy edge in the UPS results. Among them, the measured width σ'_{UPS} is the convolution of the intrinsic HOMO width of the material (σ_{UPS}) and the instrument broadening factor (σ_{INS}), which can be described as $\sigma'_{UPS} = \sqrt{{\sigma_{UPS}}^2 + {\sigma_{INS}}^2}$. In this paper, σ_{INS} is determined by measuring the Fermi edge of clean Ag, and thus, by decoupling σ_{INS}, the HOMO width of each HTL is derived.

Supplementary Note 3

The conductivity calculation method

The conductivity is calculated by fitting the *I-V* curves using the Drude model.

$$\sigma_C = \frac{d}{AR} \quad (2)$$

where σ_C represents the conductivity, d represents the thickness of the NiO_x/PTAA layer, A represents the active area of device and R represents the resistance

obtained from the *I-V* curve of device.

Supplementary Note 4

The method for calculating defect density and hole mobility via space charge limited current (SCLC) characterization.

In the *I-V* characterization curve, the low bias region is the ohmic region, the medium bias region is the defect filling limit region, and the high bias region is the SCLC region. The boundary between the low bias region and the medium bias region is the defect filling limit voltage (V_{TFL}), and the defect density (N_t) is obtained by Eq. 3.

$$N_t = \frac{2\varepsilon\varepsilon_0 V_{TFL}}{eL^2} \tag{3}$$

Where ε is the vacuum permittivity, ε_0 is the relative permittivity of the perovskite, e is the electron charge, and L is the thickness of the perovskite film.

The carrier mobility can be calculated from the SCLC area according to the Mott-Gurney law in Eq. 1.

Supplementary Note 5

The basic formula for conductivity in P-type semiconductors is shown in Eq. 4.

$$\sigma_C = p \times q \times \mu_p \tag{4}$$

where σ_C represents the conductivity, p represents the hole concentration, q represents the charge of the electron and μ_p represents the hole mobility.

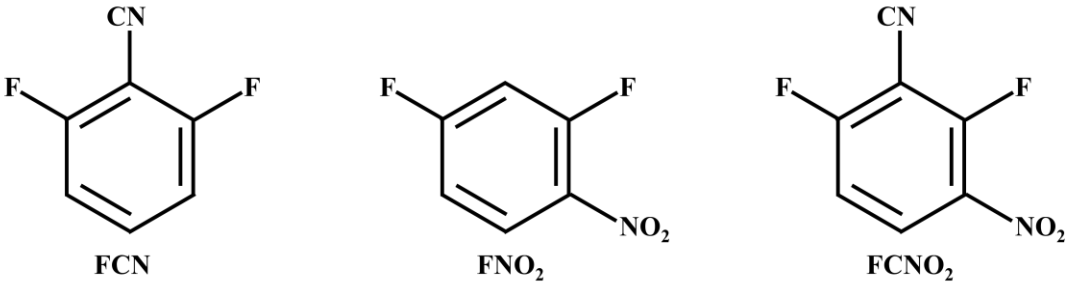

Figure S1. Chemical structure and of FCN, FNO_2, $FCNO_2$ molecules.

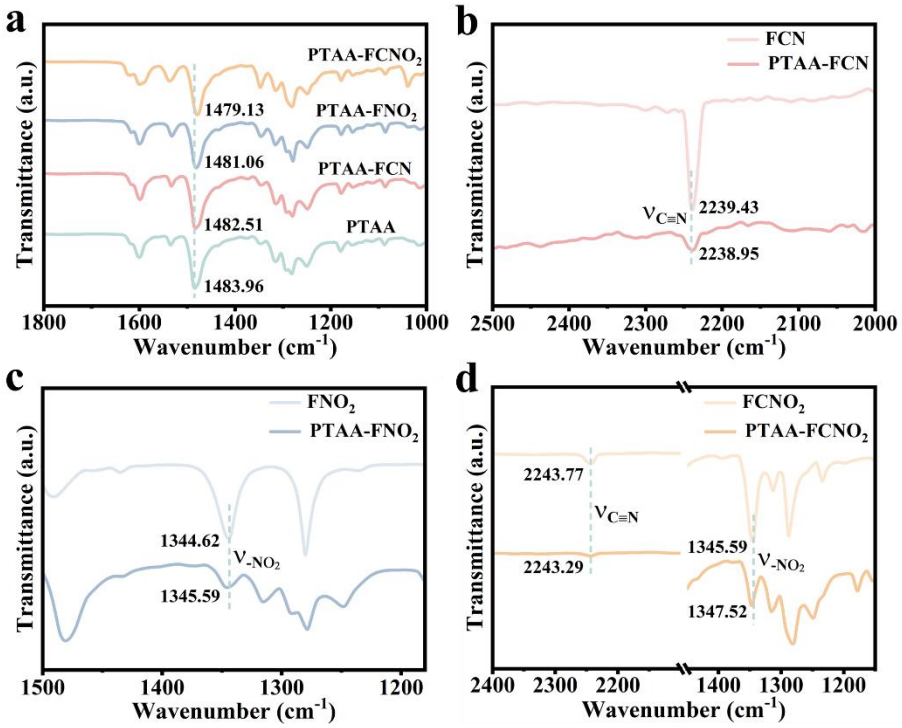

Figure S2. a) FT-IR spectra of PTAA and PTAA incorporated with FCN, FNO_2 and $FCNO_2$. FT-IR spectra of b) FCN and FCN-incorporated PTAA, c) FNO_2 and FNO_2-incorporated PTAA and d) $FCNO_2$ and $FCNO_2$-incorporated PTAA.

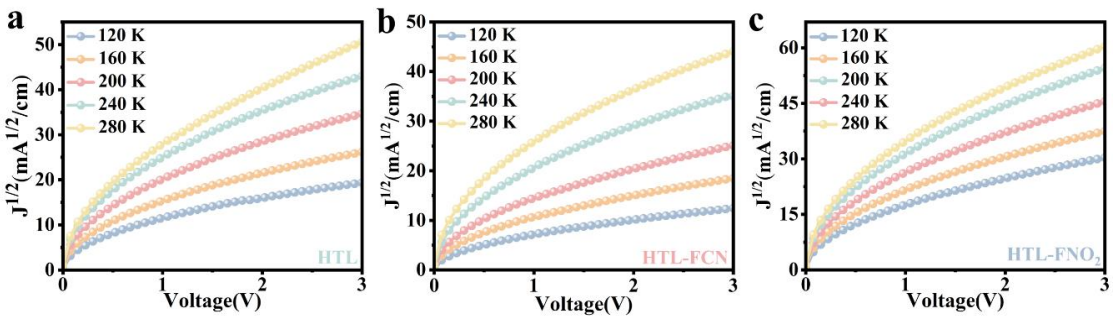

Figure S3. Hole mobility characterizations of a) pristine HTL, b) FCN-incorporated HTL and c) FNO_2-incorporated HTL at different temperatures

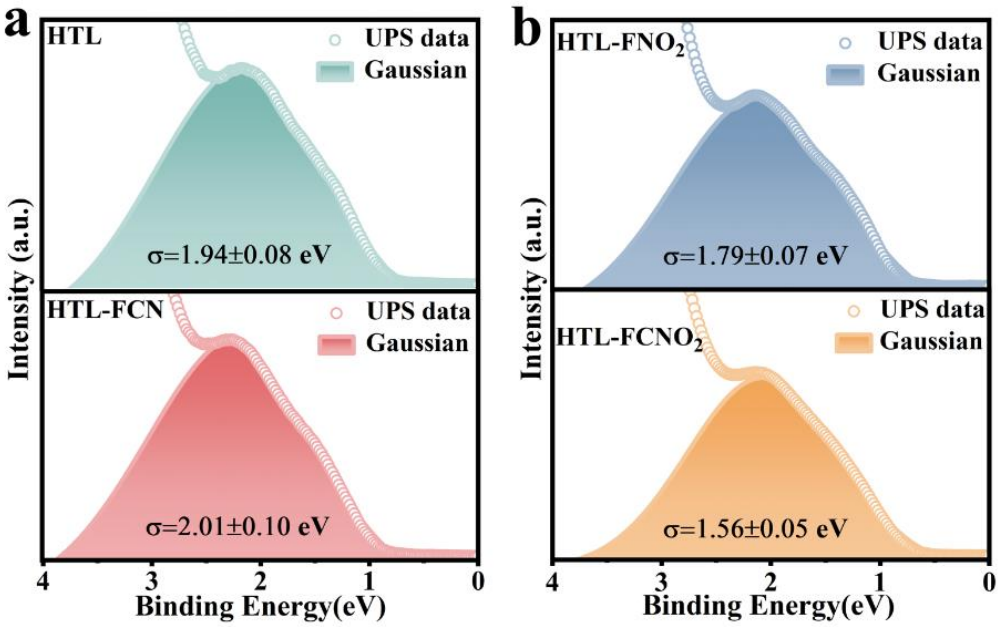

Figure S4. Gaussian fitting of the HOMO energy levels of (a) pristine HTL and FCN-incorporated HTL, (b) FNO_2-incorporated HTL and $FCNO_2$-incorporated HTL

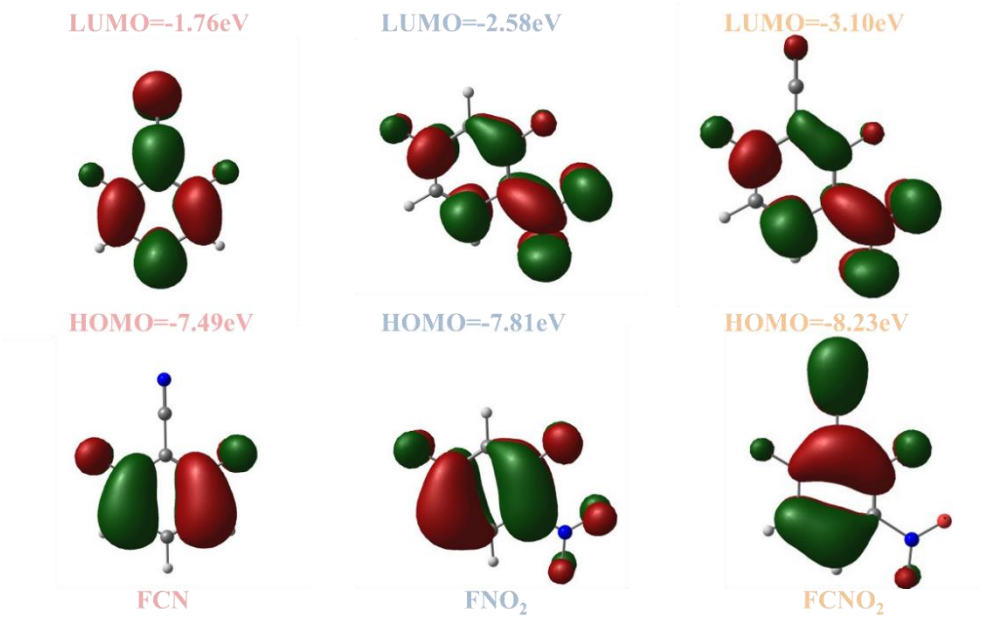

Figure S5. Schematic of LUMO and HOMO of a) FCN, b) FNO_2, c) $FCNO_2$ molecules, calculated by DFT (B3LYP, 6-31G*).

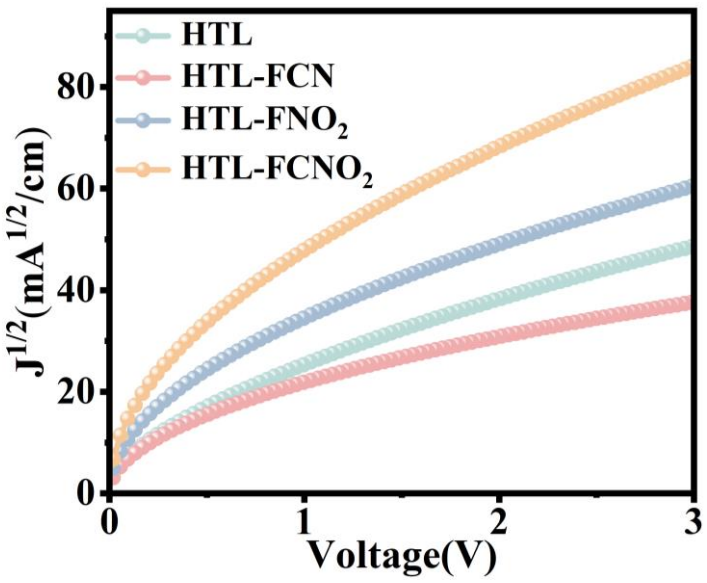

Figure S6. Hole mobility of pristine HTL, FCN-incorporated HTL, FNO_2-incorporated HTL and $FCNO_2$-incorporated HTL.

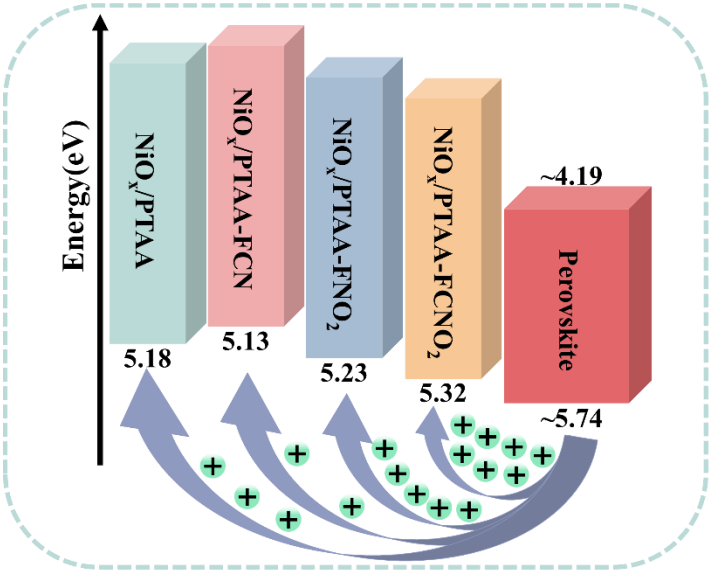

Figure S7. Schematic diagram of hole injection from perovskite into HTL.

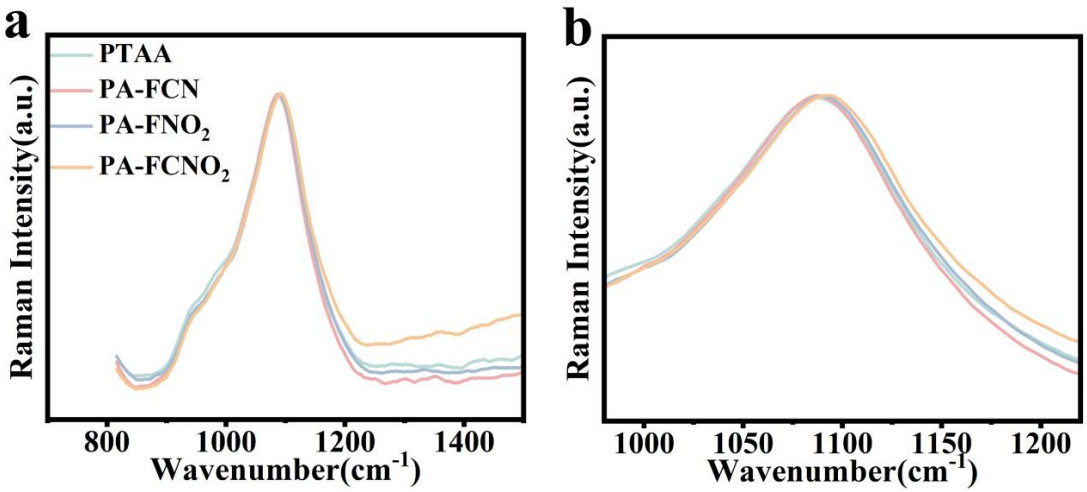

Figure S8. a) Raman spectra of PTAA, FCN-incorporated PTAA, FNO_2-incorporated PTAA and $FCNO_2$-incorporated PTAA at 1100 cm^{-1}. b) Locally enlarged Raman spectra at 1100 cm^{-1}. (PA refers to PTAA)

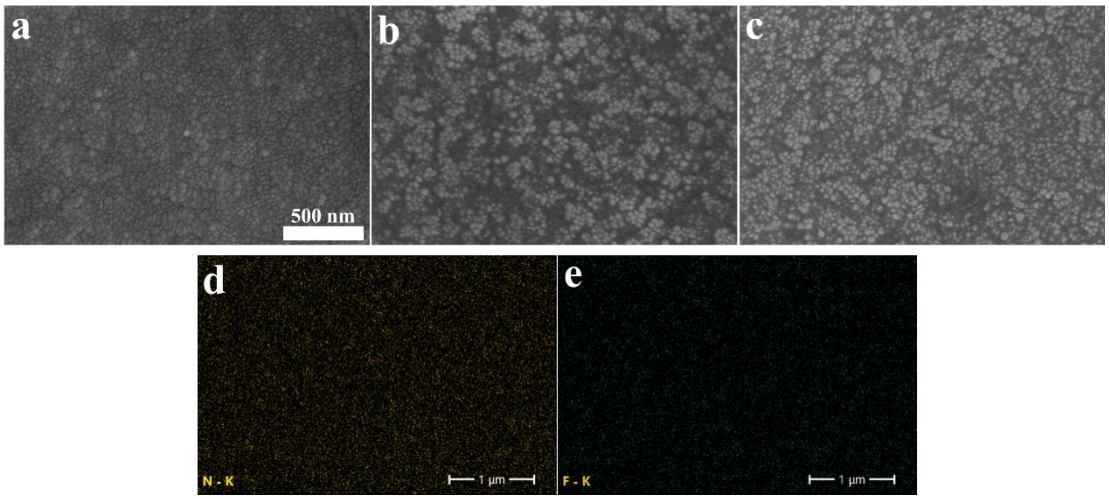

Figure S9. SEM images of a) NiO_x film, b) NiO_x/PTAA film and c) $FCNO_2$-incorporated NiO_x/PTAA film. The element mapping analysis of $FCNO_2$-incorporated NiO_x/PTAA film: d) N and e) F.

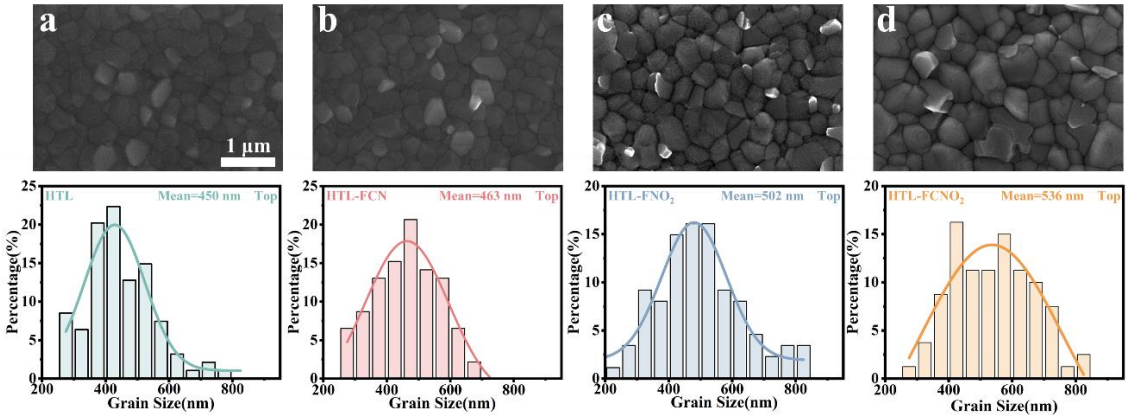

Figure S10. Top-view SEM images and Histogram of grain size distribution of perovskite films deposited on a) HTL, b) FCN-incorporated HTL, c) FNO_2-incorporated HTL and d) $FCNO_2$-incorporated HTL.

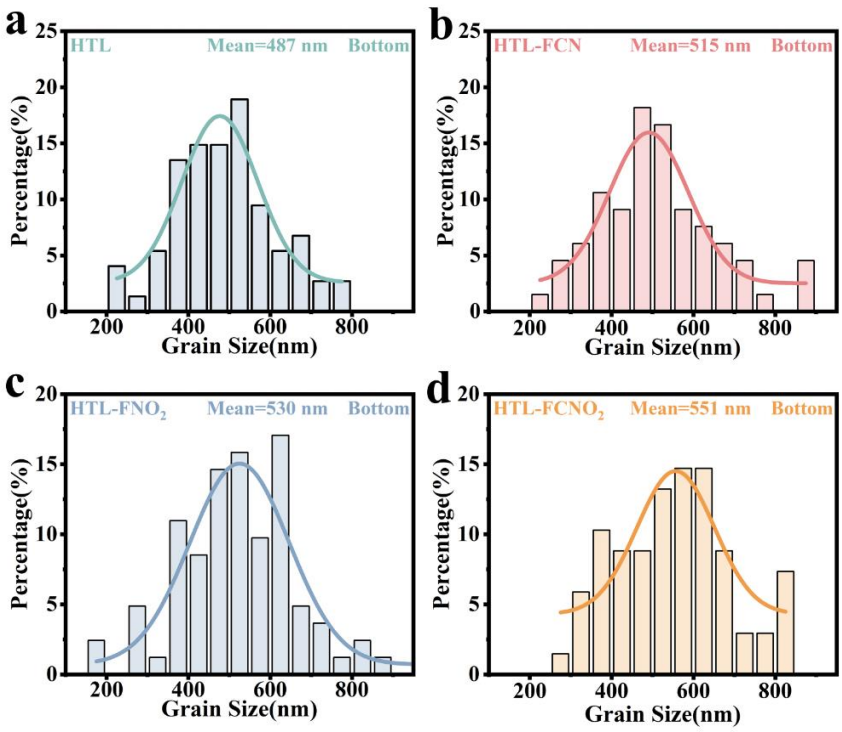

Figure S11. Histogram of grain size distribution corresponding to bottom surface SEM of perovskite films deposited on a) HTL, b) FCN-incorporated HTL, c) FNO_2-incorporated HTL and d) $FCNO_2$-incorporated HTL.

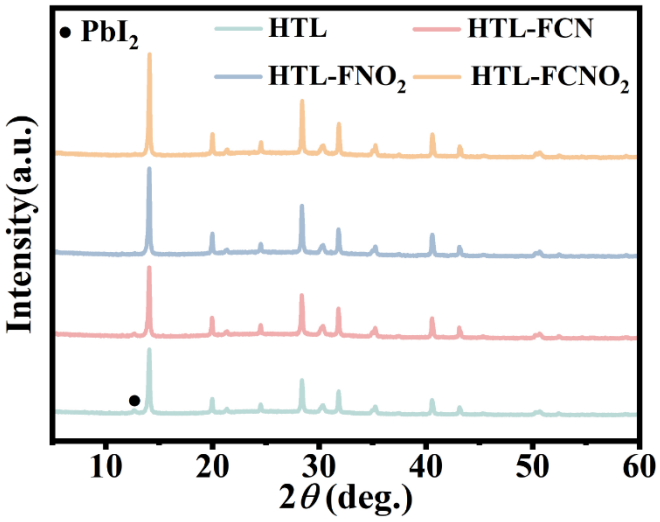

Figure S12. XRD patterns of the perovskite films deposited on HTL, FCN-incorporated HTL, FNO_2-incorporated HTL and $FCNO_2$-incorporated HTL

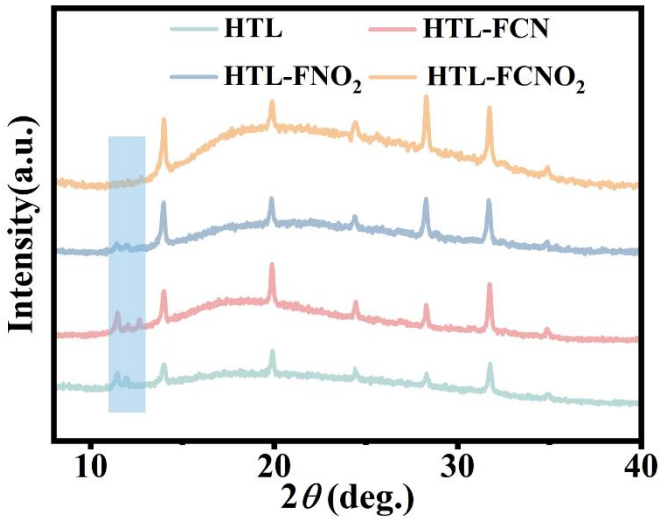

Figure S13. Bottom surface XRD patterns of perovskite films deposited on HTL, FCN-incorporated HTL, FNO_2-incorporated HTL and $FCNO_2$-incorporated HTL.

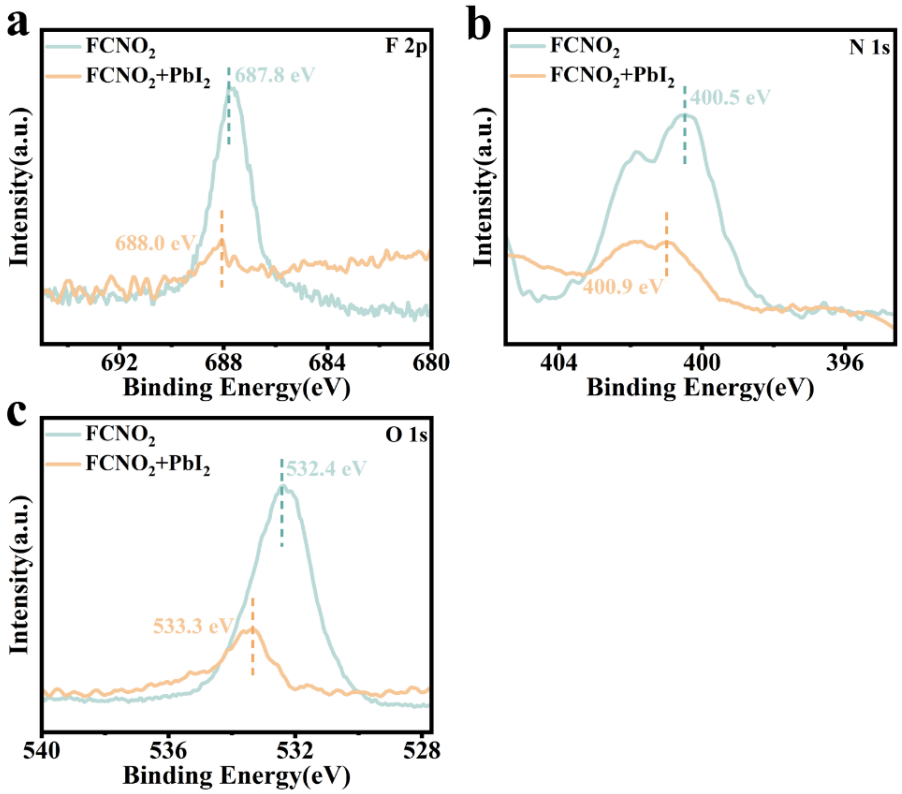

Figure S14. XPS of a) F 2p, b) N 1s and c) O 1s for $FCNO_2$ and $FCNO_2$+PbI_2.

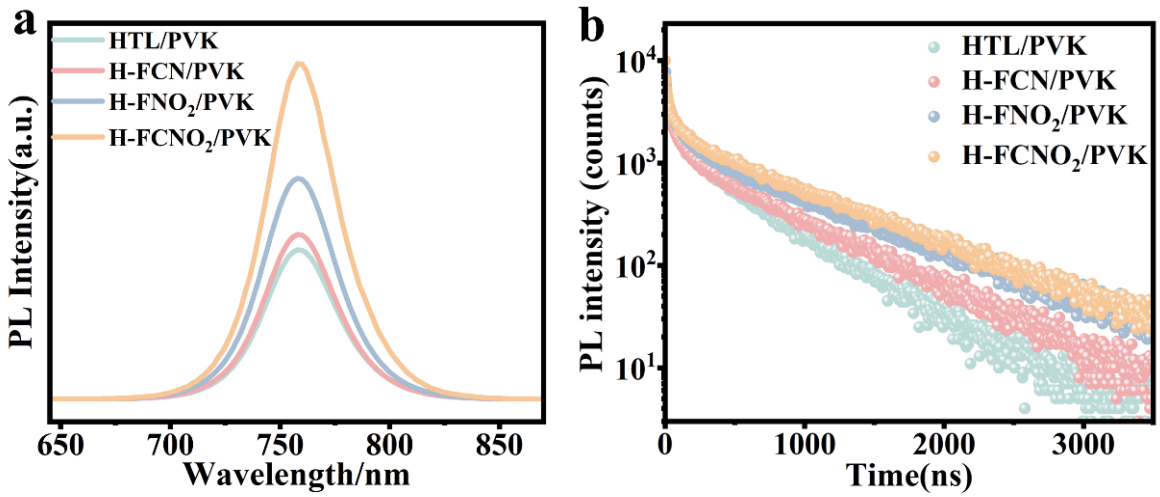

Figure S15. a) Steady-state PL spectra and b) time-resolved PL spectra of perovskite films deposited on different types of HTLs, irradiating fluorescence from the side of the perovskite film. (H refers to HTL)

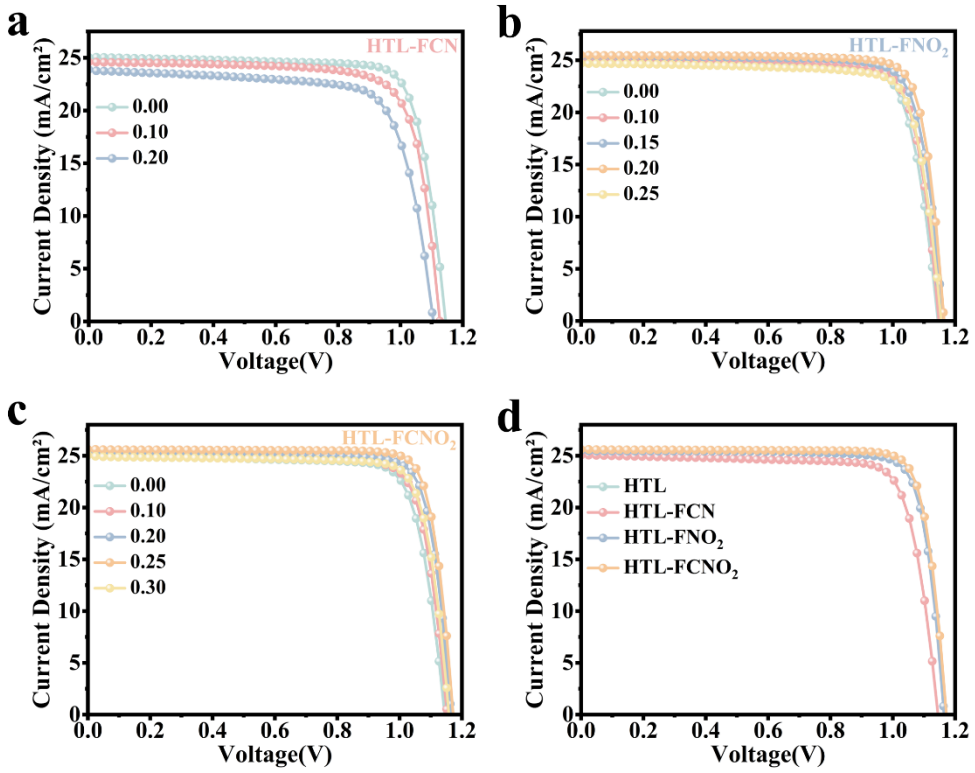

Figure S16. *J-V* curves of devices prepared with HTLs incorporated by different concentrations of a) FCN, b) FNO_2 and c) $FCNO_2$ (mg/mL). d) *J-V* curves of devices obtained from HTL incorporated with optimal concentrations of FCN, FNO_2 and $FCNO_2$.

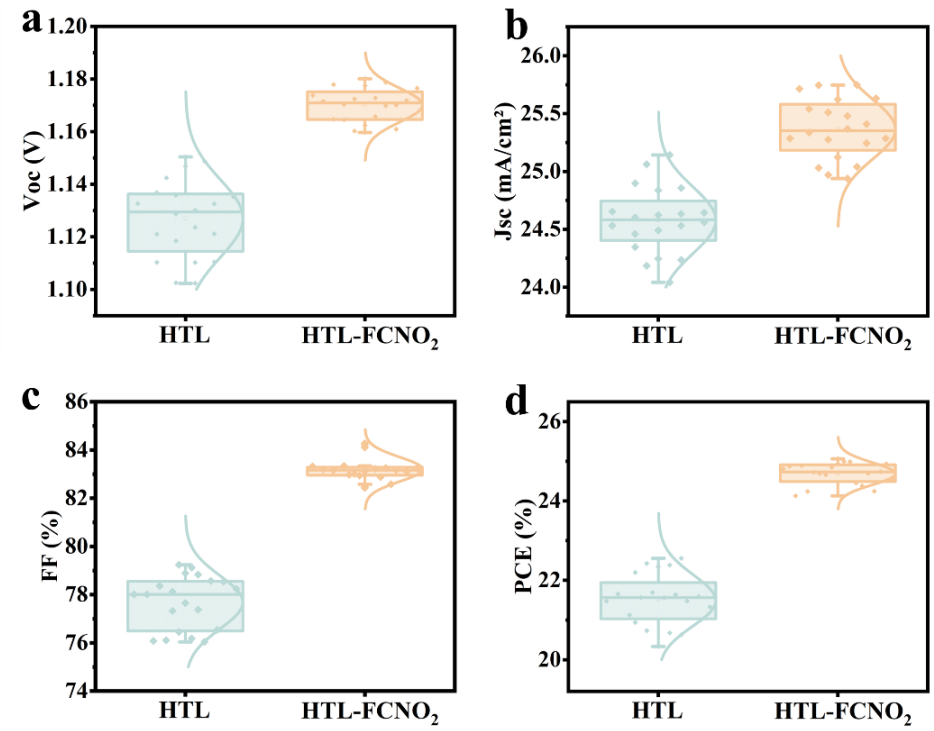

Figure S17. a) V_{oc}, b) J_{sc}, c) FF, and d) PCE statistical diagrams of the control device and $FCNO_2$-incorporated device (photovoltaic parameters from 20 devices).

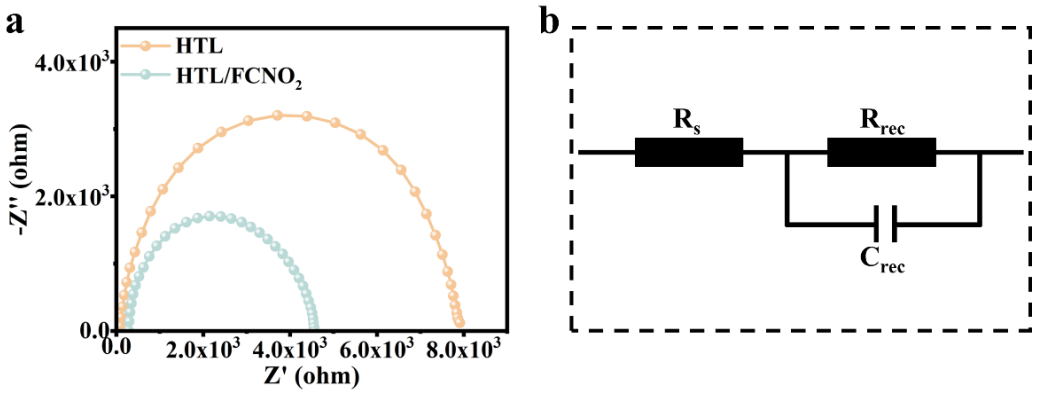

Figure S18. a) Nyquist plot characteristics of the control and $FCNO_2$-incorporated devices. b) The equivalent circuit model for EIS fitting.

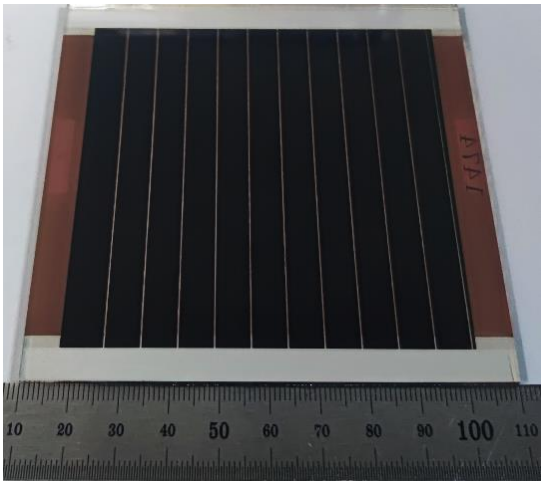

Figure S19. The physical picture of perovskite solar module.

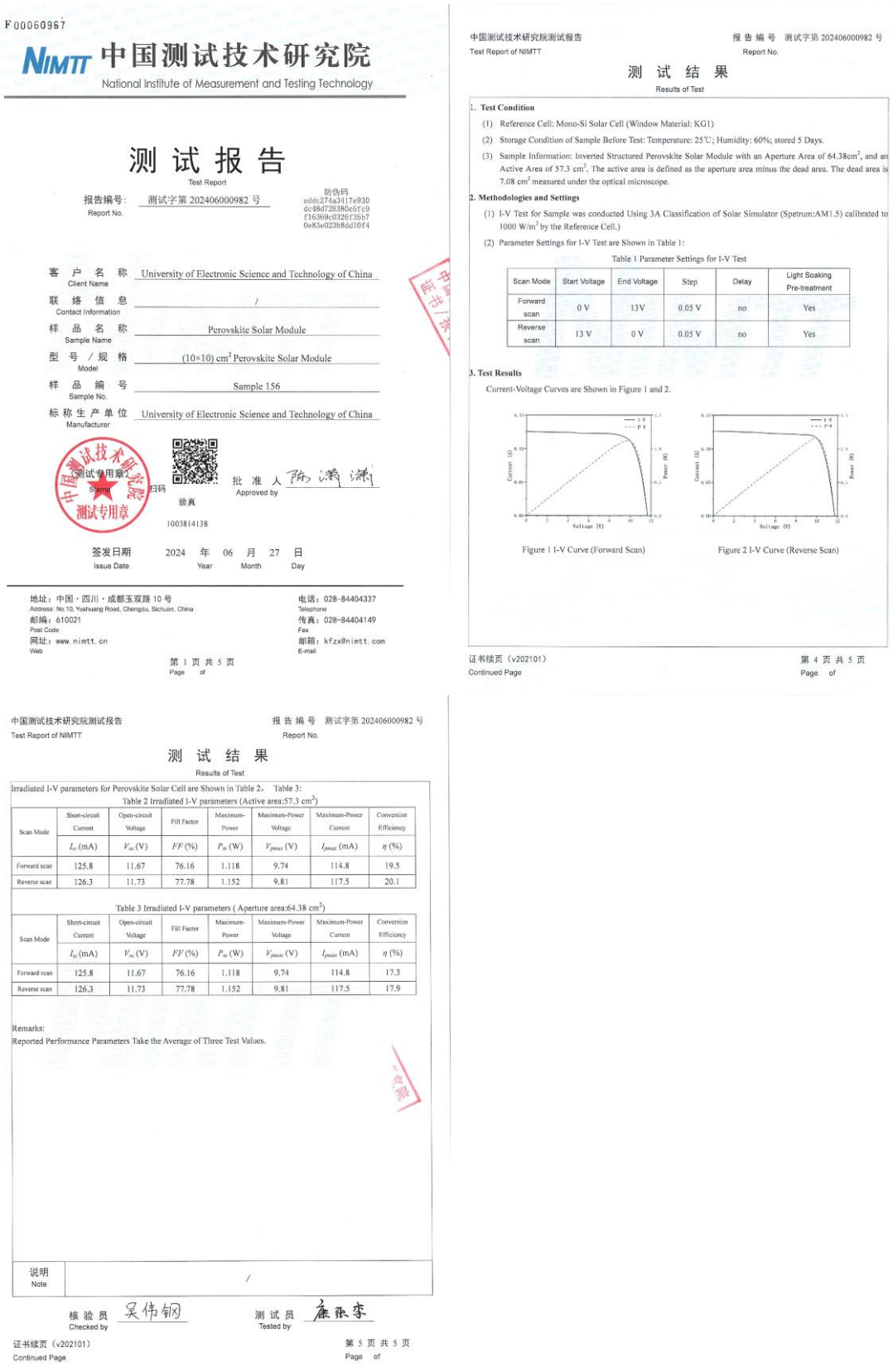

F00060967

NIMTT 中国测试技术研究院

National Institute of Measurement and Testing Technology

测 试 报 告

Test Report

报告编号: 测试字第 202406000982 号

Report No.

防伪码

nddc274a3417e930
dc48d726380e5fc9
f16369e0326f35b7
0e83e023b8dd10f4

客 户 名 称 Client Name: University of Electronic Science and Technology of China

联 络 信 息 Contact Information: /

样 品 名 称 Sample Name: Perovskite Solar Module

型 号 / 规 格 Model: (10×10) cm^2 Perovskite Solar Module

样 品 编 号 Sample No.: Sample 156

标称生产单位 Manufacturer: University of Electronic Science and Technology of China

测试专用章 Stamp

扫码

验真

1003814138

批 准 人 Approved by: 陈满琳

签发日期 Issue Date: 2024 年 Year 06 月 Month 27 日 Day

地址：中国·四川·成都玉双路 10 号
Address: No.10, Yushuang Road, Chengdu, Sichuan, China
邮编：610021
Post Code
网址：www.nimtt.cn
Web

电话：028-84404337
Telephone
传真：028-84404149
Fax
邮箱：kfzx@nimtt.com
E-mail

第 1 页 共 5 页
Page of

中国测试技术研究院测试报告
Test Report of NIMTT

报告编号 测试字第 202406000982 号
Report No.

测 试 结 果

Results of Test

1. Test Condition

(1) Reference Cell: Mono-Si Solar Cell (Window Material: KG1)

(2) Storage Condition of Sample Before Test: Temperature: 25℃; Humidity: 60%; stored 5 Days.

(3) Sample Information: Inverted Structured Perovskite Solar Module with an Aperture Area of 64.38cm^2, and an Active Area of 57.3 cm^2. The active area is defined as the aperture area minus the dead area. The dead area is 7.08 cm^2 measured under the optical microscope.

2. Methodologies and Settings

(1) I-V Test for Sample was conducted Using 3A Classification of Solar Simulator (Spetrum:AM1.5) calibrated to 1000 W/m^2 by the Reference Cell.)

(2) Parameter Settings for I-V Test are Shown in Table 1:

Table 1 Parameter Settings for I-V Test

Scan Mode	Start Voltage	End Voltage	Step	Delay	Light Soaking Pre-treatment
Forward scan	0 V	13V	0.05 V	no	Yes
Reverse scan	13 V	0 V	0.05 V	no	Yes

3. Test Results

Current-Voltage Curves are Shown in Figure 1 and 2.

Figure 1 I-V Curve (Forward Scan)

Figure 2 I-V Curve (Reverse Scan)

证书续页（v202101）
Continued Page

第 4 页 共 5 页
Page of

中国测试技术研究院测试报告
Test Report of NIMTT

报告编号 测试字第 202406000982 号
Report No.

测 试 结 果

Results of Test

Irradiated I-V parameters for Perovskite Solar Cell are Shown in Table 2, Table 3:

Table 2 Irradiated I-V parameters (Active area:57.3 cm^2)

Scan Mode	Short-circuit Current	Open-circuit Voltage	Fill Factor	Maximum-Power	Maximum-Power Voltage	Maximum-Power Current	Conversion Efficiency
	I_{sc} (mA)	V_{oc} (V)	FF (%)	P_m (W)	V_{pmax} (V)	I_{pmax} (mA)	η (%)
Forward scan	125.8	11.67	76.16	1.118	9.74	114.8	19.5
Reverse scan	126.3	11.73	77.78	1.152	9.81	117.5	20.1

Table 3 Irradiated I-V parameters (Aperture area:64.38 cm^2)

Scan Mode	Short-circuit Current	Open-circuit Voltage	Fill Factor	Maximum-Power	Maximum-Power Voltage	Maximum-Power Current	Conversion Efficiency
	I_{sc} (mA)	V_{oc} (V)	FF (%)	P_m (W)	V_{pmax} (V)	I_{pmax} (mA)	η (%)
Forward scan	125.8	11.67	76.16	1.118	9.74	114.8	17.3
Reverse scan	126.3	11.73	77.78	1.152	9.81	117.5	17.9

Remarks:
Reported Performance Parameters Take the Average of Three Test Values.

说明 Note	/

核验员 Checked by: 吴伟钢

测试员 Tested by: 康孙李

证书续页（v202101）
Continued Page

第 5 页 共 5 页
Page of

Figure S20. The certified PCE of $FCNO_2$-incorporated perovskite photovoltaic module (*J-V* characterization). The report is issued by NIMTT (National Institute of Measurement and

Testing Technology). The active area is 57.3 cm^2 measured by NIMTT.

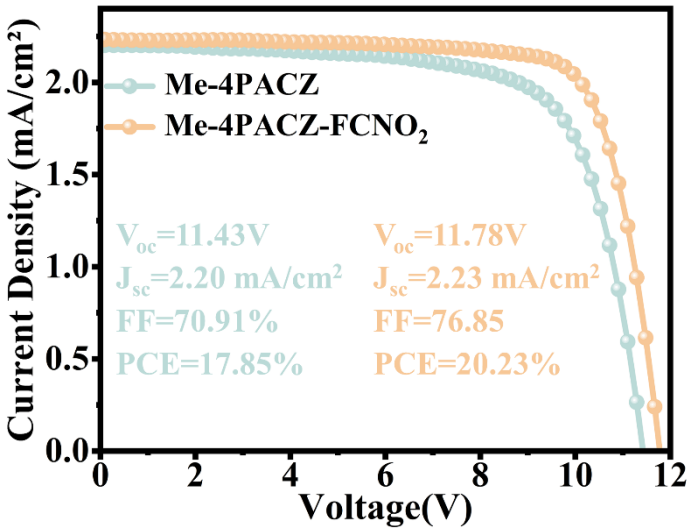

Figure S21. *J-V* curve and corresponding photovoltaic parameters of NiO_x/Me-4PACZ based PSMs without and with $FCNO_2$.

Table S1. The PL decay curves of perovskite films deposited on different HTLs substrates fitted by a bi-exponential decay equation of $I(t) = I_0 + A_1\exp(-t/\tau_1) + A_2\exp(-t/\tau_2)$, and average time constant $(\tau_{ave}) = (A_1\tau_1^2 + A_2\tau_2^2)/(A_1\tau_1 + A_2\tau_2)$, with irradiating fluorescence incident from the glass side.

Sample	τ_1(ns)	τ_2(ns)	τ_{ave}(ns)
HTL	3.77	136.16	125.09
HTL-FCN	3.21	138.52	129.54
HTL-FNO_2	3.05	100.19	91.51
HTL-$FCNO_2$	1.84	58.87	52.89

Table S2. The PL decay curves of perovskite films deposited on different HTLs substrates fitted by a bi-exponential decay equation of $I(t) = I_0 + A_1\exp(-t/\tau_1) + A_2\exp(-t/\tau_2)$, and average time constant $(\tau_{ave}) = (A_1\tau_1^2 + A_2\tau_2^2)/(A_1\tau_1 + A_2\tau_2)$, with irradiating fluorescence incident from the side of the perovskite film.

Sample	τ_1(ns)	τ_2(ns)	τ_{ave}(ns)
HTL	15.17	321.89	285.72
HTL-FCN	15.01	438.70	390.50
HTL-FNO_2	17.43	568.52	524.83
HTL-$FCNO_2$	18.71	656.26	606.08

Table S3. Photovoltaic parameters of PSCs based on unmodified HTL, optimal concentrations of FCN, FNO_2 and $FCNO_2$-incorporated HTL.

Device	V_{oc}[V]	J_{sc}[mA/cm^2]	FF	PCE[%]
HTL	1.14	25.06	78.74	22.50
HTL-FCN	1.14	25.06	78.74	22.50
HTL-FNO_2	1.16	25.49	82.17	24.30
HTL-$FCNO_2$	1.17	25.62	83.23	25.01

Table S4. Photovoltaic parameters extracting from *J-V* curves for the best-performing NiO_x/PTAA-based inverted control and $FCNO_2$-incorporated devices

Device	Scan	V_{oc}[V]	J_{sc}[mA/cm^2]	FF	PCE[%]	HI
Control	FS	1.141	25.08	73.34	20.96	0.068
	RS	1.142	25.06	78.74	22.50	
HTL-$FCNO_2$	FS	1.170	25.55	82.72	24.72	0.012
	RS	1.173	25.62	83.23	25.01	

Table S5. Summary of photovoltaic performance of reported high-efficiency inverted PSMs up to now. (active area over 50 cm^2)

Device structure	active area (cm^2)	PCE [%]	Certified PCE (%)	Ref.
FTO/NiO_x/$FCNO_2$-PTAA/Perovskite/C_{60}/BCP/Cu	**57.3**	**20.6**	**20.1**	**This work**
FTO/NiO_x/Perovskite-urea/C_{60}/BCP/Cu	61.56	20.56	–	Nano-Micro Lett, 2024, 16:190
ITO/NiO_x/PEAI/Perovskite/DMATFA/PCBM/BCP/Ag	63.74	20.58	–	Adv. Mater, 2024, 36, 2313860
ITO/PTAA/Perovskite-Zn-additives/C_{60}/BCP/Ag	79.67	19.97	19.60	Nat. Commun, 2024, 15:13551
FTO/NiO_x/Perovskite-L-AA/C_{60}/BCP/Cu	57.3	19.17	–	ACS Appl. Mater. Interfaces, 2024, 16, 4751-4762
ITO/Urea-NiO_x/Perovskite/BzMIMBr/C_{60}/BCP/Cu	178.4	17.18	–	Adv. Funct. Mater. 2023, 33, 2214774
FTO/NiO_x with SRE/Perovskite/PC_{61}BM/BCP/Ag	174	18.6	–	Joule, 2022, 6, 1931-1943
ITO/PTAA/Perovskite/C_{60}/BCP/Cu	50.1	19.7	19.15	Science, 2021, 373, 902-907